JGR Oceans

RESEARCH ARTICLE

Key Points:

- A hypothesis that a wind feedback contributes to Arctic Amplification is rejected by performing dedicated wind perturbation simulations
- Winter sea ice retreat in the northern Barents Sea causes anomalous cyclonic winds by locally enhancing ocean heat loss
- Anomalous cyclonic winds result in less Atlantic Water transport through Fram Strait

Impact of Cyclonic Wind Anomalies Caused by Massive Winter Sea Ice Retreat in the Barents Sea on Atlantic Water Transport Toward the Arctic: A Model Study

Finn Ole Heukamp[1] , **Torsten Kanzow[1,2]** , **Qiang Wang[1]** , **Claudia Wekerle[1]** , and **Rüdiger Gerdes[1,3]**

[1]Alfred-Wegener-Institute, Helmholtz Center for Polar and Marine Research, Bremerhaven, Germany, [2]University of Bremen, Bremen, Germany, [3]Jacobs-University Bremen, Bremen, Germany

Abstract The Arctic is warming much faster than the global average. This is known as Arctic Amplification and is caused by feedbacks in the local climate system. In this study, we explore a previously proposed hypothesis that an associated wind feedback in the Barents Sea could play an important role by increasing the warm water inflow into the Barents Sea. We find that the strong recent decrease in Barents Sea winter sea ice cover causes enhanced ocean-atmosphere heat flux and a local air temperature increase, thus a reduction in sea level pressure and a local cyclonic wind anomaly with eastward winds in the Barents Sea Opening. By investigating various reanalysis products and performing high-resolution perturbation experiments with the ocean and sea ice model FESOM2.1, we studied the impact of cyclonic atmospheric circulation changes on the warm Atlantic Water import into the Arctic via the Barents Sea and Fram Strait. We found that the observed wind changes do not significantly affect the warm water transport into the Barents Sea, which rejects the wind-feedback hypothesis. At the same time, the cyclonic wind anomalies in the Barents Sea increase the amount of Atlantic Water recirculating westwards in Fram Strait by a downslope shift of the West Spitsbergen Current, and thus reduce Atlantic Water reaching the Arctic basin via Fram Strait. The resulting warm-water anomaly in the Greenland Sea Gyre drives a local anticyclonic circulation anomaly.

Plain Language Summary The Barents Sea has been experiencing a rapid decrease in its winter sea ice extent during the last 30 years. The loss of sea ice creates new areas where, in winter, the relatively warm ocean loses heat to the cold atmosphere. As warm air rises, the warming reduces the sea level air pressure, changing the atmospheric circulation to develop a local anticlockwise wind system centered over the northern Barents Sea. The associated eastward winds in the Barents Sea Opening and southeastward winds in Fram Strait affect how warm water from the North Atlantic moves toward the Arctic. There has been a long debate on whether this wind anomaly can increase the warm Atlantic Water transport into the Barents Sea and thus cause a positive feedback mechanism for further reducing the sea ice through melting. We find that the observed atmospheric circulation changes have no significant impact on the Barents Sea warm water inflow and thus reject the wind feedback as a strong player in contributing to Arctic Amplification. However, strong anomalous southeastward winds in Fram Strait and the northern Nordic Seas cause a southward shift of the warm Atlantic Water recirculation and reduce its flow toward the Arctic.

1. Introduction

One of the fastest-changing regions of the Arctic is the Barents Sea, located north of Norway between Svalbard, Franz Josef Land, and Novaya Zemlya. Although covering only about 10% of the Arctic Ocean area, the Barents Sea is of Arctic-wide importance because the warm water advected from the North Atlantic causes massive heat fluxes into the atmosphere and sea ice melt, ultimately driving major water mass modifications relevant for the Arctic Ocean circulation and heat budget downstream (e.g., Gerdes et al., 2003; Serreze et al., 2007; Smedsrud et al., 2013; Dmitrenko et al., 2015). As part of the upper limb of the Atlantic Meridional Overturning Circulation, warm and saline Atlantic Water enters the Barents Sea via the Norwegian Atlantic Current/Norwegian Coastal Current (Figure 1). In comparison to the second Atlantic Water branch entering the Arctic Ocean via the deep Fram Strait, the shallow Barents Sea facilitates mixing, thus exposing the Atlantic Water very efficiently to the cold polar atmosphere, which results in large ocean-atmosphere heat fluxes in winter (Smedsrud et al., 2010). Hence, on its pathway through the Barents Sea, the Atlantic Water cools down to almost the freezing point and

Writing – review & editing: Finn Ole Heukamp, Torsten Kanzow, Qiang Wang, Claudia Wekerle, Rüdiger Gerdes

thereby releases most of the heat (76 TW, in the climate condition of the 20th century, Smedsrud et al., 2013) before being insulated from the atmosphere and ice interactions by the Cold Arctic Halocline, a subsurface layer of cold and fresh water (Steele et al., 1995). Due to its extraordinary role in the exchange of heat, the Barents Sea is considered the "cooling machine" of the Arctic. Its role as a cooling machine is however changing in a warming climate (Shu et al., 2021; Skagseth et al., 2020).

The exchange of heat between the ocean and the atmosphere naturally varies and is directly linked to the extent of the winter sea ice cover. While high-frequency atmosphere variability (e.g., transient cyclones) impacts the Barents Sea sea ice extent on timescales of several days (Aue et al., 2022; Boisvert et al., 2016; Graham et al., 2019; Schreiber & Serreze, 2020), Lien et al. (2017) showed that Atlantic Water variability contributes to sea ice anomalies from sub-seasonal to longer timescales. It is still debated whether interannual to decadal variations in the Barents Sea ice cover are mainly driven by variability of the Atlantic Water heat transport (Årthun et al., 2012, 2019; Wang et al., 2019) or variability of the atmospheric circulation (Liu et al., 2022; Sorteberg & Kvingedal, 2006).

The Barents Sea winter sea ice cover has pronounced natural multi-year variability, with events of pronounced sea ice gain followed by events of pronounced sea ice loss (e.g., Årthun et al., 2019; Bonan et al., 2021; England et al., 2019). In addition, recent observations and model studies found rapid changes in the Barents Sea heat content as well as in the extent of winter sea ice (e.g., Barton et al., 2018; Cavalieri & Parkinson, 2012; Comiso et al., 2008; Lind et al., 2018; Onarheim & Årthun, 2017; Screen & Simmonds, 2010) making the Barents Sea a hotspot for the extraordinary warming of the Arctic. Over the last four decades, the Barents Sea has experienced ocean warming (Ingvaldsen et al., 2004) as a result of warming in the Atlantic Water (Wang et al., 2019) accompanied by a reduction in winter sea ice cover to less than a third of the pre-satellite mean (Onarheim & Årthun, 2017). In future climate projections, the Barents Sea is estimated to be ice-free in winter within the time period 2061–2088 (Onarheim & Årthun, 2017).

The retreat of Barents Sea winter sea ice is suggested to affect both remote (Yang & Christensen, 2012; Yang et al., 2016) and local atmospheric circulation patterns (Ådlandsvik & Loeng, 1991; Smedsrud et al., 2013). Focusing on local effects, the coupled ocean-atmosphere-ice system may as a whole form a positive wind feedback mechanism (e.g., Bengtsson et al., 2004; Lien et al., 2017; Smedsrud et al., 2013; Ådlandsvik & Loeng, 1991) involving ocean heat transport, sea ice cover, heat fluxes, and atmospheric circulation changes. If this feedback is active, it may significantly contribute to the above-average warming of the Arctic known as Arctic Amplification.

A schematic of the wind feedback is shown in Figure 2. An initial positive perturbation in the Atlantic Water heat transport toward the Barents Sea leads to a warmer Barents Sea. Due to the additional oceanic heat, less winter sea ice is formed and there is increased net surface heat loss from the ocean to the atmosphere (Figure 2b). The increased ocean surface heat loss warms the lower atmosphere (Figure 2c). The warmer air rises, causing near-surface atmospheric convergence which results in a local reduction of sea level pressure (Figure 2d). This reduction in sea level pressure drives a cyclonic atmospheric circulation anomaly that goes along with westerly winds over the Barents Sea Opening (Figure 2d). The additional winds cause anomalous Ekman transport out of the central Barents Sea toward the Norwegian coast. The resulting increase in the meridional sea surface height (SSH) gradient may then increase the transport of warm Atlantic Water into the Barents Sea via an acceleration of the geostrophic currents (Figure 2e). The increased Atlantic Water transport into the Barents Sea then closes the positive feedback loop as additional oceanic heat is available for further sea ice melt and the initial anomaly is amplified.

The nature of coupled feedbacks makes it difficult to disentangle causes and effects in observational data. To date, only a few modeling attempts have been made to assess this possible feedback. Ådlandsvik and Loeng (1991) postulated two stable climate states for the Barents Sea, a warm and a cold state. According to their study, the warm phase is characterized by reduced sea ice, increased Atlantic Water inflow, and increased sea surface heat loss. They hypothesized the Barents Sea wind feedback to maintain the stability of the warm phase and thus regarded the feedback as a relevant contribution to Barents Sea climate variability. However, their results are based on an early regional 17-year model study and the postulation of the feedback is rather speculative than based on evidence. In contrast, Smedsrud et al. (2013) found no evidence for the wind feedback in a 600-year fully coupled run of a climate model. However, their coarse resolution model (about 90 km grid spacing in the Barents Sea) may not be able to resolve the branched Atlantic Water flow into the Barents Sea and its sensitivity to local winds.
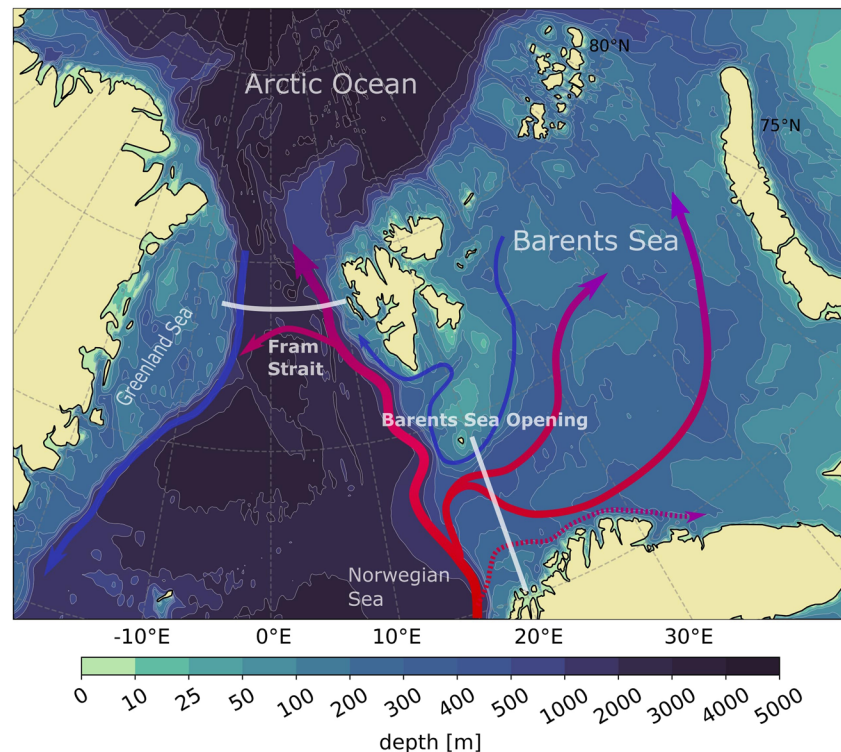
Figure 1. Atlantic Water pathways into the Arctic via Barents Sea Opening and Fram Strait. Red arrows depict warm Atlantic Water, blue lines depict cold Polar Water. The dashed line represents the Norwegian Coastal Current.

The second main source of oceanic heat in the Arctic is the West Spitzbergen Current that transports warm and saline Atlantic Water through Fram Strait (Aagaard & Greisman, 1975; Aagaard et al., 1987). The West Spitsbergen Current bifurcates near 79°N into one branch that continues flowing north toward the central Arctic basins, and a second branch that turns westward to form a recirculation that feeds the eastern flank of the cold and fresh southward-directed East Greenland Current (e.g., Bourke et al., 1987, 1988). According to De Steur et al. (2014), about 50% (2.7 Sv) of the Atlantic Water recirculates southwards in Fram Strait. Due to the pronounced impact of the recirculation on the amount of Atlantic Water that reaches the Arctic Ocean, changes in its strength and location may significantly affect the oceanic heat transport toward the Arctic. Moreover, the modification of the polar waters in the East Greenland Current by the intrusion of recirculating Atlantic Water forms the main source of the Denmark Strait Overflow (Strass et al., 1993) and hence affects the deep southward flow of the Atlantic Meridional Overturning Circulation.

Fram Strait is also the major gateway of the Arctic for the export of sea ice with an annual mean export of about 880,000 km^2 (roughly 10% of the Arctic sea ice area). Sea ice export through Fram Strait contributes to freshwater export into the Nordic Seas. The sea ice area export rate is increasing by about 6% per decade as the general increase of the sea level pressure difference between Greenland and Spitsbergen generates enhanced meridional winds (Smedsrud et al., 2017). In contrast, sea ice volume export through Fram Strait is decreasing due to Arctic sea ice thinning (Spreen et al., 2020; Wang et al., 2021). In this regard, Wang et al. (2020) demonstrated that the general decline of the Arctic sea ice results in an intensification of the Atlantic Water supply to the Arctic Ocean via a steric decrease of sea surface height in the Nordic Seas due to less sea ice meltwater.

To prove the existence of the Barents Sea wind feedback mechanism, all processes in the feedback loop need to be verified. However, even if only one process within the feedback loop shown in Figure 2 does not work, the hypothesis of the existence of the feedback mechanism can already be rejected. In this study, we conduct several high-resolution simulations with the state-of-the-art ocean and sea ice model FESOM2.1 to investigate whether cyclonic wind anomalies in the Barents Sea can increase the Atlantic Water inflow through the Barents Sea Opening so that it can potentially initiate the positive feedback contributing to Arctic Amplification. That is, we will focus on the process from Figures 2d–2e. If we can demonstrate that this particular process does not occur, we can conclude that the feedback mechanism illustrated in Figure 2 does not function effectively.
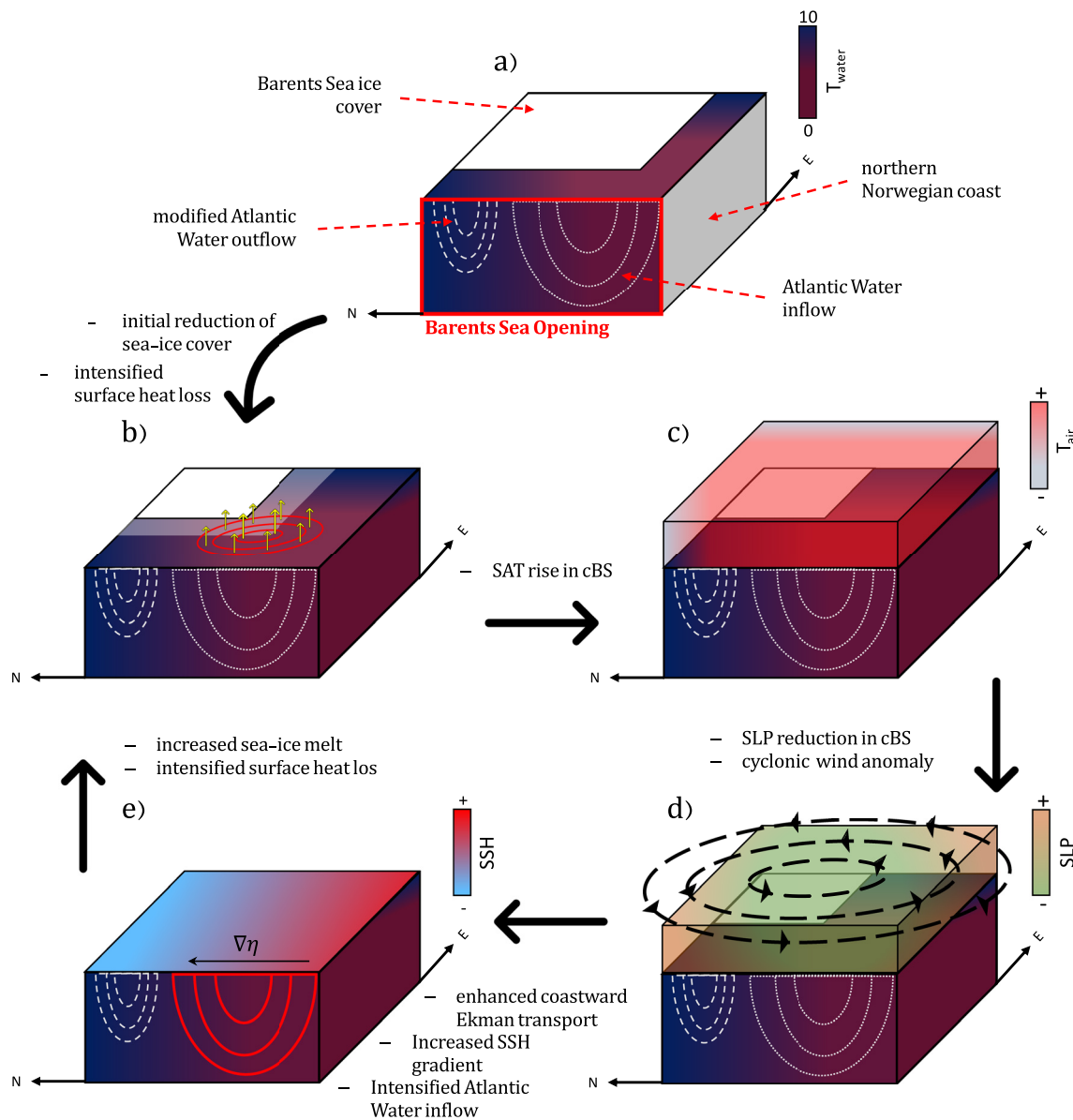
Figure 2. Schematic of the Barents Sea wind feedback. Abbreviations: sea level pressure (SLP), surface air temperature (SAT), central Barents Sea (cBS), sea surface height (SSH). In this study we rejected this previously hypothesized feedback using model simulations.

Understanding whether this feedback mechanism is at play is crucial because of the strong implication on Arctic climate change.

We have two main tasks in this paper. First, we will use wind perturbation simulations to investigate whether the above-described wind feedback exists. Second, we will use numerical simulations to understand whether these wind perturbations can significantly influence ocean circulation in Fram Strait.

2. Data and Methods

2.1. Model Setup, Control Simulation, and Validation

To investigate the proposed wind feedback in the Barents Sea we use the unstructured-mesh ocean and sea ice model FESOM2.1 (Danilov et al., 2017). FESOM2 and its precursor FESOM1 have already been used by, for example, Wekerle et al. (2013), Wekerle, Wang, von Appen et al. (2017), Wekerle, Wang, Danilov et al. (2017), and Wang et al. (2018, 2019) to investigate various processes in the Arctic. In contrast to many common ocean

models, FESOM2.1 is formulated on triangular meshes. This unstructured-mesh approach allows for locally refining the horizontal resolution, avoiding unwanted effects that come along with nesting approaches on classical grids. We use a global mesh with ∼4.5 km grid resolution in the whole Arctic domain including the Nordic Seas and about 25 km north of 40°N outside the Arctic. Vertically, the model is split into 45 layers with a layer thickness of 10 m close to the surface, increasing to 250 m in the deep ocean.

The model was started from rest with temperature and salinity conditions from PHC3 (Steele et al., 2001). First, we performed a spin-up in which the model was forced with CORE1 normal year forcing (Large & Yeager, 2009), a climatological one-year annual cycle of 6-hourly atmospheric forcing without interannual variability that was repeated every year. After a spin-up of 40 years, the monthly mean Barents Sea Opening Atlantic Water transport has reached a quasi-equilibrium without pronounced interannual variability. We continue with the simulation for eight years, which is referred to as the control simulation. The control simulation reasonably reproduces sea ice cover, hydrographic properties, and transports in the Barents Sea Opening and Fram Strait, compared to observational sections presented by Lien et al. (2016) (their Figure 6) and Beszczynska-Möller et al. (2012) (their Figure 3). During the winter months (December–May) the location of the isoline of the 95% sea ice concentration in our control simulation is in good agreement with the monthly mean sea ice concentration from NSIDC from 1979 to 1999 (Figure 3). Mean winter sections along 20°E (Barents Sea Opening) and 78.8°N (Fram Strait) are presented in Figure 4. In the central Barents Sea Opening warm ($T > 5°C$) and saline Atlantic Water enters the Barents Sea while, close to Bear Island, modified Atlantic Water is transported out of the Barents Sea via a strong westward current at the Bear Island slope (Figures 1 and 4). On the Bear Island shelf, polar waters are found and temperatures rapidly decrease toward the north. Close to the Norwegian coast in the vicinity of the Norwegian Coastal Current waters are slightly cooler than the central Atlantic Water inflow but salinity rapidly decreases toward the coast due to the large coastal freshwater inflow (Figures 4a–4c). We further observe an annual mean net Barents Sea Opening transport of 2.7 Sv (Figure 4d), which is within the observational range of 0.8–2.9 Sv (Beszczynska-Möller et al., 2011) and slightly exceeds the annual mean of 2.0 Sv provided by Smedsrud et al. (2010). The Barents Sea Opening net transport shares the same seasonal variability as in the observations with increased transport during winter and minimum transport in early summer (Årthun et al., 2012).

In Fram Strait, our model reasonably reproduces the general circulation pattern with the sluggish barotropic northward flow of warm and saline Atlantic Water in the eastern part of the basin that is intensified at the upper continental slope of Svalbard in the West Spitsbergen Current. In the western part, the flow is directed southward and peaks in the broad and surface intensified flow of the East Greenland Current. Water masses in the East Greenland Current are cold and fresh and vertical stratification is dominated by salinity. Moreover, the model reproduces the thick Atlantic Water layer between the surface and about 700 m depth with temperatures exceeding 2°C and salinities above 34.9 PSU (Figures 4e–4g). The net transport across Fram Strait in the model is about −2 Sv (Figure 4h), which well reproduced the observational estimate (−2 ± 2.7 Sv, Schauer et al. (2008)).

Given the reasonable performance of the control simulation, we can then use the sensitivity experiments to explore the ocean response to cyclonic wind perturbations.

2.2. Perturbation Experiments

We run wind-perturbation experiments by adding cyclonic wind anomalies to the wind forcing in the Barents Sea area. The wind-perturbation simulations are the same as the control simulation, except that we superimpose spatially confined wind anomalies onto the normal year forcing. The wind anomalies are added constantly and do not change seasonally. The difference in the model results between the wind-perturbation simulations and the control simulation can reveal the impact of wind perturbations on ocean circulation.

One version of wind anomalies is generated by subtracting the mean winter (December–May) sea level pressure of the recent period 2000–2019 from the historical period 1979–1999 using the JRA55-do reanalysis (Kobayashi et al., 2015). The other version is generated similarly but takes the recent period of 2000–2009 using the NCEP-CORE2 reanalysis (Large & Yeager, 2009). These sea level pressure anomalies are then converted to geostrophic wind fields. The winds are computed based on an f-plane at 75°N and are spatially bounded by the
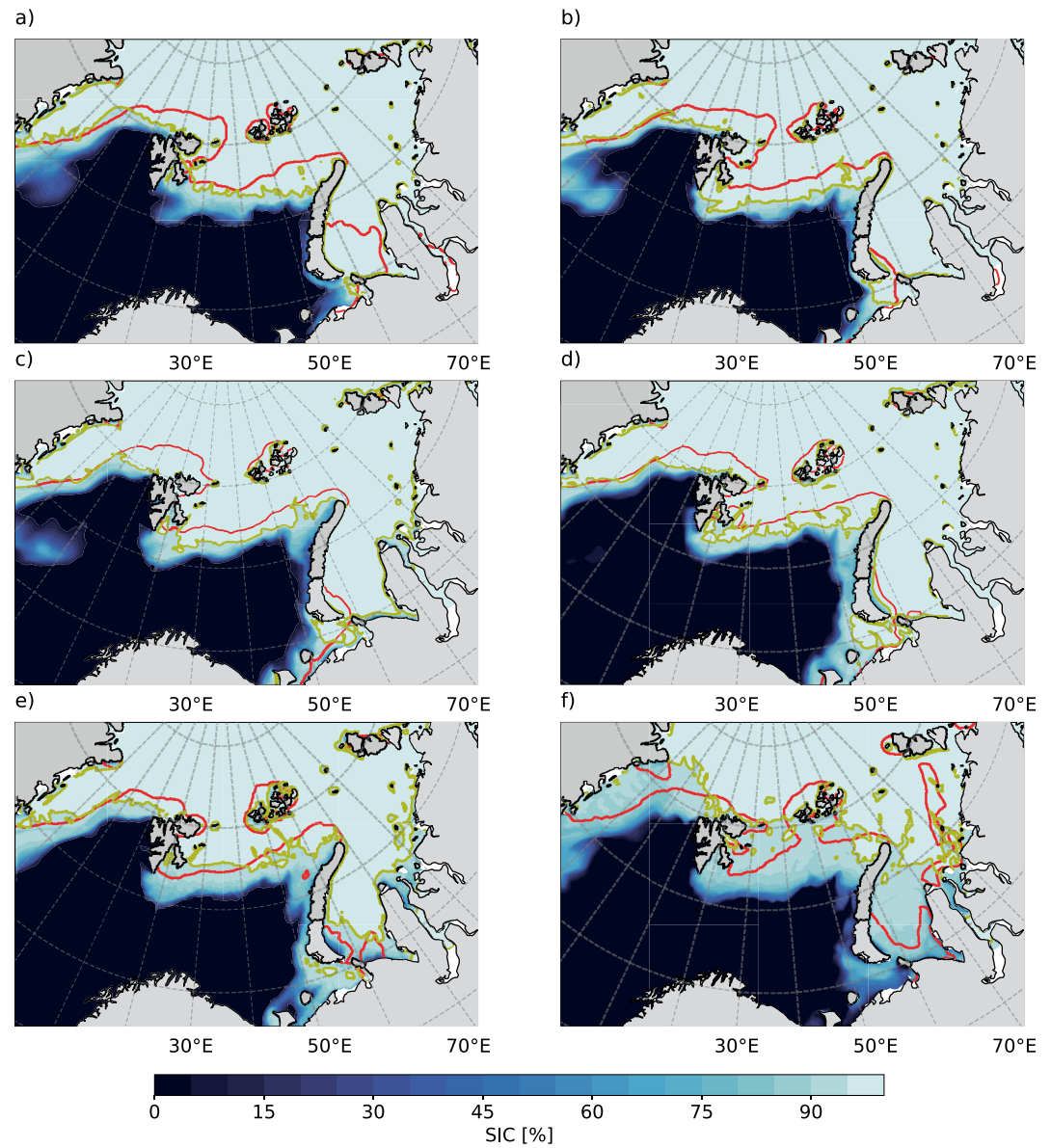
Figure 3. Monthly mean sea ice concentration in the control simulation for (a) December, (b) January, (c) February, (d) March, (e) April, and (f) May, averaged over the 8 years of the control simulation. Yellow lines represent monthly mean 95% sea ice concentration. Red lines depict the 95% isoline of the 1979–1999 monthly mean sea ice concentration from NSIDC data.

coast of Greenland and the 90°E meridian and 70°N and 85°N latitudes. To account for the effect of surface friction the resulting winds are deflected and scaled according to Proshutinsky and Johnson (1997):

$$
\begin{pmatrix} u \\ v \end{pmatrix} = 0.7 \times \begin{pmatrix} u_{geo} \\ v_{geo} \end{pmatrix} \times \begin{bmatrix} \cos(30°) & -\sin(30°) \\ \sin(30°) & \cos(30°) \end{bmatrix}
$$

where (u, v) represents the corrected 10 m wind velocities and (u_{geo}, v_{geo}) represents the initially computed geostrophic winds. The final wind anomalies that are added to the CORE1 winds in the perturbation runs are shown in Figures 5d and 5e. The wind perturbations form a cyclonic pattern in the Barents Sea that covers the Barents Sea Opening and Fram Strait.
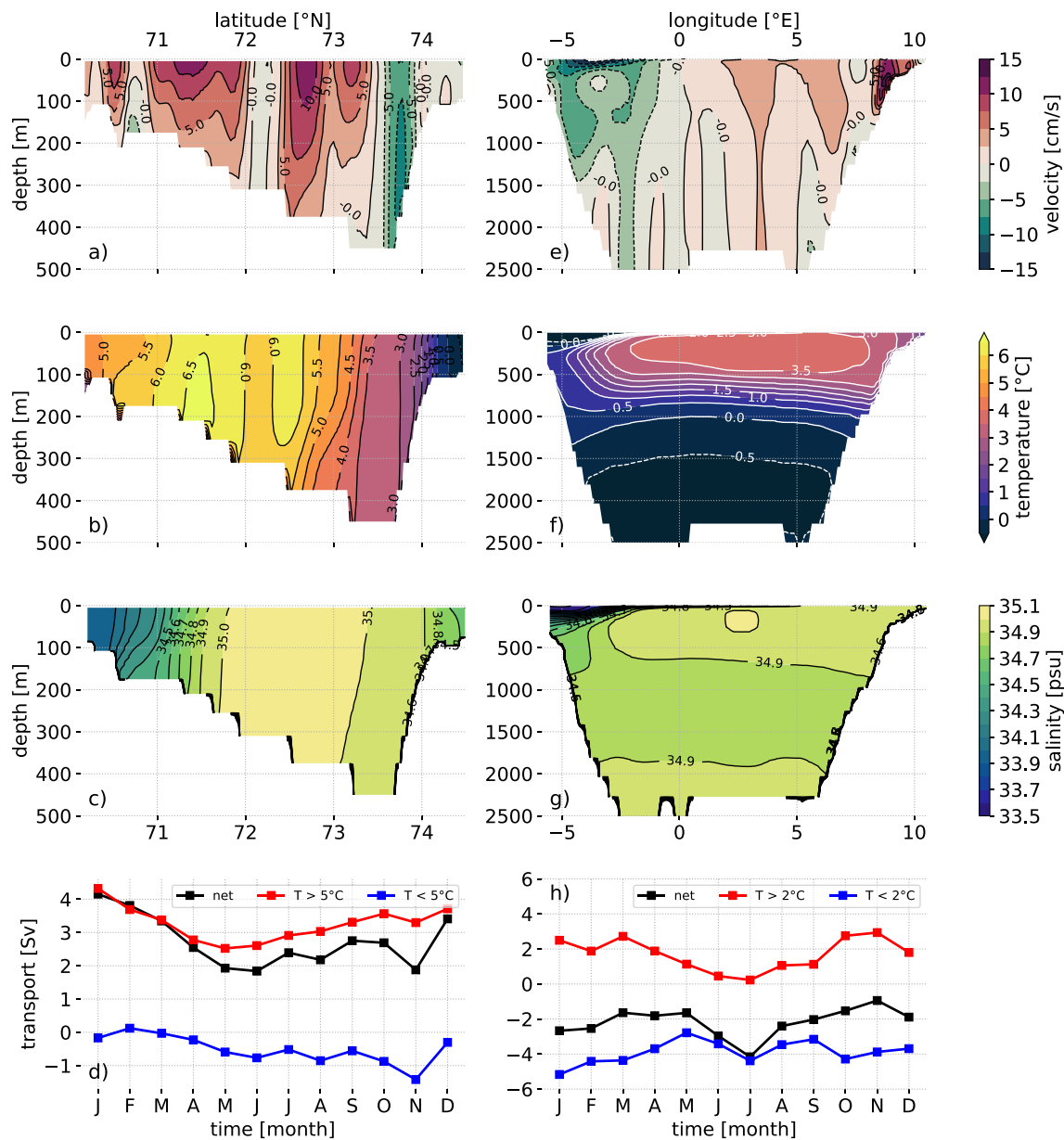
Figure 4. Winter (December–May) (a) mean zonal velocity, (b) temperature, (c) and salinity in the section along Barents Sea Opening (20°E, 70°–74.5°N) as well as (e) mean winter meridional velocity, (f) temperature, and (g) salinity in the section across Fram Strait (78.8°N, 6°W–10.5°E). Monthly mean transport in CTRL through (d) Barents Sea Opening and (h) Fram Strait with and without temperature limitations.

3. Results

3.1. Changes in the Barents Sea Winter Mean State

Several components of the Barents Sea climate system are rapidly changing. Without the sea ice cover, the Barents Sea loses more heat and moisture to the atmosphere in winter. The enhanced winter heat loss of the ocean leads to local warming of the atmosphere. Warm and moist air replaces cool and dry air masses. These developments can be observed by comparing the Arctic winter (December–May) mean state of the period 1979–1999 and 2000–2018 (2000–2009). Maps of the difference in sea ice concentration, surface air temperature, and sea level pressure (Figure 5) were derived based on the National Snow and Ice Data Center (NSIDC) monthly mean data for sea ice concentration, and the JRA55 and NCEP-CORE2 (NCEP) reanalysis for surface air temperature and sea level pressure. The most pronounced Arctic winter sea ice loss has
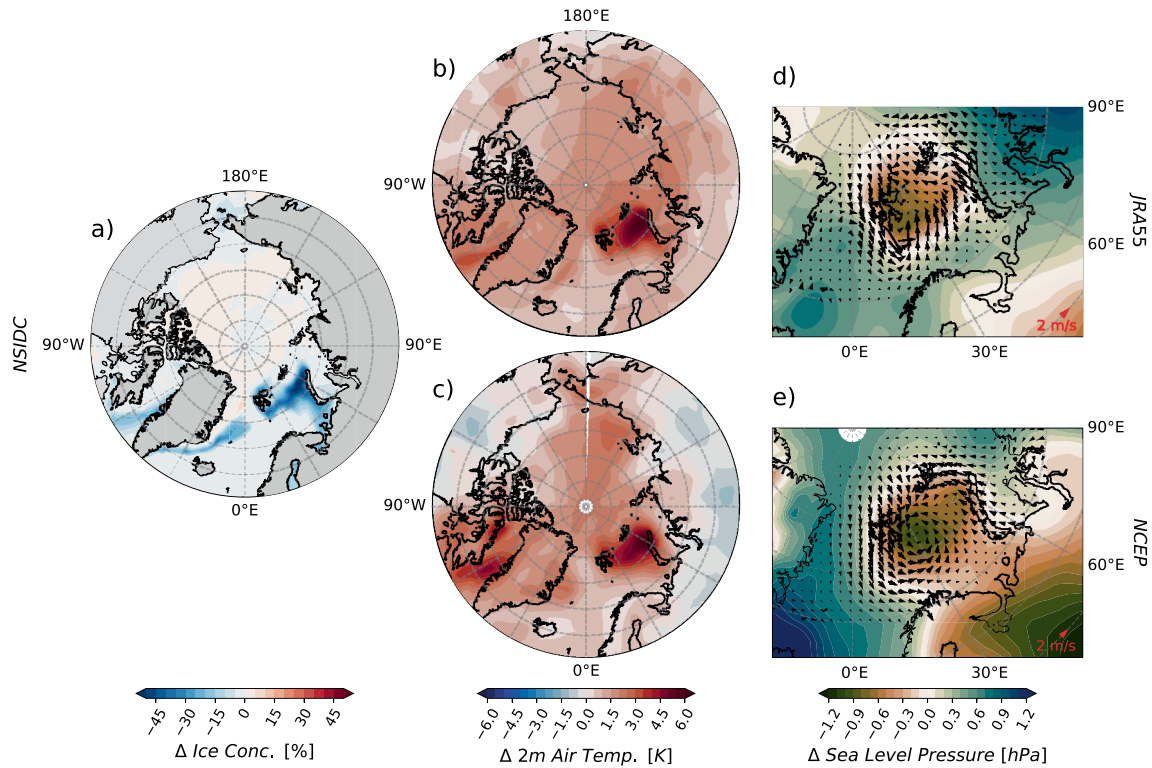
Figure 5. Difference in the winter (December–May) Arctic mean state (JRA55-do: 2000–2015 minus 1979–1999, CORE2: 2000–2009 minus 1979–1999) for: (a) sea ice concentration from NSIDC data; (b, c), surface air temperature; (d, e) sea level air pressure. The vector fields in (d and e) represent geostrophic wind field anomalies computed from the sea level pressure anomalies that are applied to perturb the model in the wind-perturbation experiments. Vectors are re-gridded for visualization; Latitude grid lines are drawn every 5°N.

occurred in the northern and north-eastern Barents Sea (Figure 5a). The sea ice loss is most pronounced along the Atlantic Water pathway west of northern Novaya Zemlya, where the sea ice concentration has decreased by up to 50%. Additional areas of enhanced sea ice decrease are observed around Spitsbergen and in the East Greenland Sea.

As a result of the retreating ice cover, both reanalysis products reveal a strong increase in surface air temperature in the Barents Sea. In comparison with the temperature rise in the Arctic in general, the locally confined warming of the Barents Sea area is extraordinarily high and unique, reaching up to 6°C in the north-eastern Barents Sea (Figures 5b and 5c). Despite some regional differences in the Arctic wide spatial distribution of the temperature changes, the reanalysis products agree fairly well on the strong air temperature increase in the Barents Sea, in both spatial distribution and amplitude. In addition, similar temporal developments are found in sea level pressure. Local sea ice and air temperature changes in the Barents Sea spatially coincide with a decrease in sea level pressure of about 1 hPa, evident in the northern Barents Sea (Figures 5d and 5e). This local reduction in sea level pressure spatially matches the warming and sea ice loss pattern, although it's maximum is not situated immediately above the main warming spot but westwards, south-east of Spitsbergen.

The processes e → b → c → d of the feedback loop in Figure 2 are, therefore, evident in historical data. The remaining question is then whether the process d → e in the feedback loop is effective in reality. Since the reduction in sea level pressure also strongly enhances the zonal sea level pressure gradient in the vicinity of the West Spitsbergen Current, an impact on the Atlantic Water flow through Fram Strait is also likely.

3.2. Impact of Cyclonic Wind Anomalies on the Barents Sea

To assess the impact of local atmospheric circulation changes in the Barents Sea on the Atlantic Water transport we performed perturbation experiments with different additional wind anomalies as described in Section 2.2 We specifically focus on the relation between a cyclonic wind anomaly and the Atlantic Water transport (Figures 2,
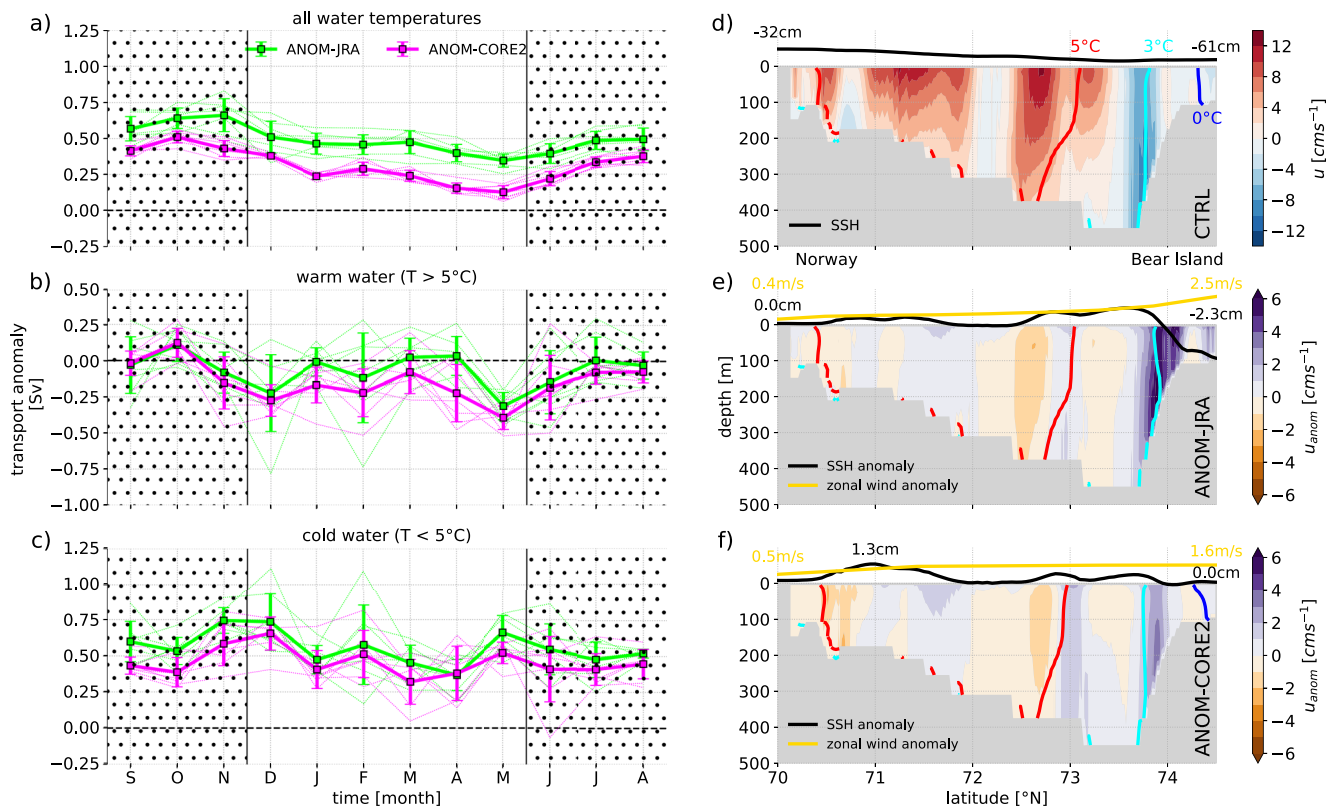
Figure 6. Barents Sea Opening transport anomaly in ANOM-JRA (green) and ANOM-CORE2 (magenta) in different temperature classes: (a) no temperature limitation, (b) $T > 5°C$, (c) $T < 5°C$. Positive value indicates an eastward anomaly. Thin lines represent single years, thick lines represent the monthly mean anomalies. Dotted areas depict summer months when the assumed wind feedback is irrelevant. All transports are computed according to Sidorenko et al. (2020). (d) Mean winter (December–May) Barents Sea Opening zonal velocity section in CTRL, as well as anomalies of the winter mean zonal velocity relative to CTRL for (e) ANOM-JRA and (f) ANOM-CORE2. Red, cyan and blue lines in (d–f) indicate the 5°C, 3°C, and 0°C isotherms in the respective runs. The thick black line qualitatively depicts the mean winter sea surface height in (d) and the sea surface height anomaly relative to CTRL in (e and f). Yellow lines in (e and f) show zonal wind anomalies (Figures 5d and 5e) along the Barents Sea Opening section. The sea surface height and wind anomalies are shown only for the purpose of understanding dynamics, and only a few values are given at specific latitudes. The results are averaged over the eight model years.

Figures 5). In the following, we refer to the CORE1 control run as CTRL, the JRA55-do perturbation run as ANOM-JRA, and the NCEP-CORE2 perturbation run as ANOM-CORE2.

To determine if the wind anomalies can close the feedback via an increase in the Barents Sea Opening warm water transport, we monitor the anomaly of the Barents Sea Opening Atlantic Water transport between the Norwegian coast and Bear Island (20°E, 70°–74.5°N) in both perturbation experiments with respect to CTRL. The monthly transport anomalies are computed for every year and split into different temperature ranges to differentiate warm Atlantic Water ($T > 5°C$) from modified Atlantic Water and Polar Water (all water masses with $T < 5°C$). The seasonal cycle of the transport anomalies is shown in Figures 6a–6c for the two different temperature ranges. Taking into account water of all temperatures, the anomaly of the Barents Sea Opening net transport indeed reveals an increase of about 0.5 Sv in ANOM-JRA and 0.3 Sv in ANOM-CORE2 (Figure 6a). Separating the transport of the warm Atlantic Water, which has the largest impact on the Barents Sea heat budget, from the transport of colder waters, we find that the increase in the net Barents Sea Opening volume transport in the perturbation simulations is not due to an increase in the warm Atlantic Water inflow but rather due to a decrease in the cold water outflow (Figures 6b and 6c). The positive transport anomaly (reduction in export) of cold water even exceeds 0.5 Sv during winter (Figure 6c). The warm Atlantic Water transport is rather slightly decreased in the perturbation runs (Figure 6b). Similar results are obtained when using the threshold of 3°C to separate the transports of warm and cold waters (not shown).

A more detailed view of changes in the mean Barents Sea Opening flow field in response to the wind perturbations is shown in Figures 6d–6f. The zonal velocity of the warm Atlantic Water in the Barents Sea Opening,

bounded by the red 5°C isotherms in Figures 6e and 6f, does not show pronounced anomalies in the perturbation runs, nor does the meridional extent of the Atlantic Water change. The circulation feature that is most affected by the additional wind forcing is the westwards-directed current south of Bear Island at 74°N, which recirculates modified Atlantic Water and Polar Water out of the Barents Sea. The additional wind forcing decelerates the westward-directed flow by 2–6 cm/s in both ANOM-JRA and ANOM-CORE2.

The changes in the currents in the Barents Sea Opening can be explained by modifications of the sea surface height gradient across the Barents Sea Opening. In CTRL (Figure 6d), the sea surface height along the Barents Sea Opening is tilted with maximum sea surface height at the Norwegian coast and minimum sea surface height near 73.5°N, yielding geostrophic Atlantic Water inflow into the Barents Sea. Further north toward Bear Island, sea surface height rises again, generating geostrophic flow out of the Barents Sea. Both the perturbation runs show a pronounced anomalous sea surface height gradient in the vicinity of the westward flow south of Bear Island, which reduces the westward flow (Figures 6e and 6f).

The sea surface height anomalies along the Barents Sea Opening can be directly attributed to the applied wind perturbations. The eastward wind anomaly in this area causes southward Ekman flow that causes a negative sea surface height gradient in the meridional direction south of Bear Island, thus producing a positive anomaly in the zonal current there (Figures 6e and 6f). Further south, the sea surface height anomaly in ANOM-JRA is rather smooth, generating hardly any anomalous flow of warm Atlantic Water into or out of the Barents Sea. In ANOM-CORE2 a pronounced sea surface height anomaly is moreover observed at 71°N, within the warm Atlantic Water flow. This causes weak westward and eastward flow anomalies which cancel out each other in terms of their impacts on Atlantic Water transport. Therefore, in both perturbation simulations, the cyclonic wind anomaly over the Barents Sea does not increase the warm Atlantic Water inflow, and the increase in the net Barents Sea Opening transport is due to the reduction in the outflow of cold waters near Bear Island. Based on these results, it seems unlikely that the wind feedback as depicted in Figure 2 can operate, as we cannot find an increase in the warm Atlantic Water import that could further decrease the sea ice extent and close the feedback loop.

To put the transport and sea surface height anomalies along the Barents Sea Opening into a broader perspective, we further look at sea surface height and sea ice concentration adaptations in the whole Barents Sea domain (Figure 7). Both ANOM-JRA and ANOM-CORE2 reveal a decrease in sea ice concentration along the sea ice edge by 20%–50% (Figures 7a and 7b). Since the air temperature is prescribed in the model and cannot adapt to changes in the ice conditions, the simulated changes in sea ice concentration in ANOM-JRA and ANOM-CORE2 can either be a result of the additional wind forcing or of melting processes from below the ice, by enhanced warm water supply. As we do not observe an increase in the Barents Sea Atlantic Water supply in the perturbation runs (Figure 4b), it seems that the sea ice concentration decrease is a direct response to the additional northward winds west of Novaya Zemlya, pushing the ice edge north (Figures 5d and 5e). A similar process is observed in Fram Strait where the additional southward winds drive enhanced sea ice export leading to an increase in sea ice concentration toward the south (Figure 7).

In comparison to CTRL, sea surface height decreases in the northern Barents Sea and increases in the southern part in the perturbation runs by 3–4 cm (Figures 5c and 5d). By decomposing the sea surface height anomalies into their steric and mass components we can address locally observed changes in sea surface height in ANOM-JRA and ANOM-CORE2 to additional meltwater from melting sea ice or wind-induced divergent/convergent Ekman flow. By applying this separation, we find that the negative sea surface height anomaly in the northern Barents Sea is mainly caused by the divergence of Ekman flow due to the additional local wind forcing as the changes in steric height are small (Figures 7c–7h). In addition to the overall small amplitude of halosteric and thermosteric height anomalies (<1 cm), their contributions partly cancel each other out in the central Barents Sea. Moreover, we do not observe a drastic change in Barents Sea sea ice meltwater flux that could change the upper ocean salinity and thus impact halosteric height, which further supports our conclusion on the dynamic origin of the Barents Sea sea surface height anomaly.

3.3. Modification of the Atlantic Water Recirculation in Fram Strait

Besides affecting the Barents Sea, the wind anomalies also significantly affect the circulation in Fram Strait, where the additional wind has a strong southward component in the vicinity of the West Spitsbergen Current, the second main Atlantic Water branch into the Arctic Ocean. As a response to the additional wind forcing there is a pronounced increase in sea surface height in Fram Strait exceeding 12 cm between 70°N and 75°N that goes along with an anticyclonic circulation anomaly (Figures 7c and 7d). Therefore, we monitor the strength of the
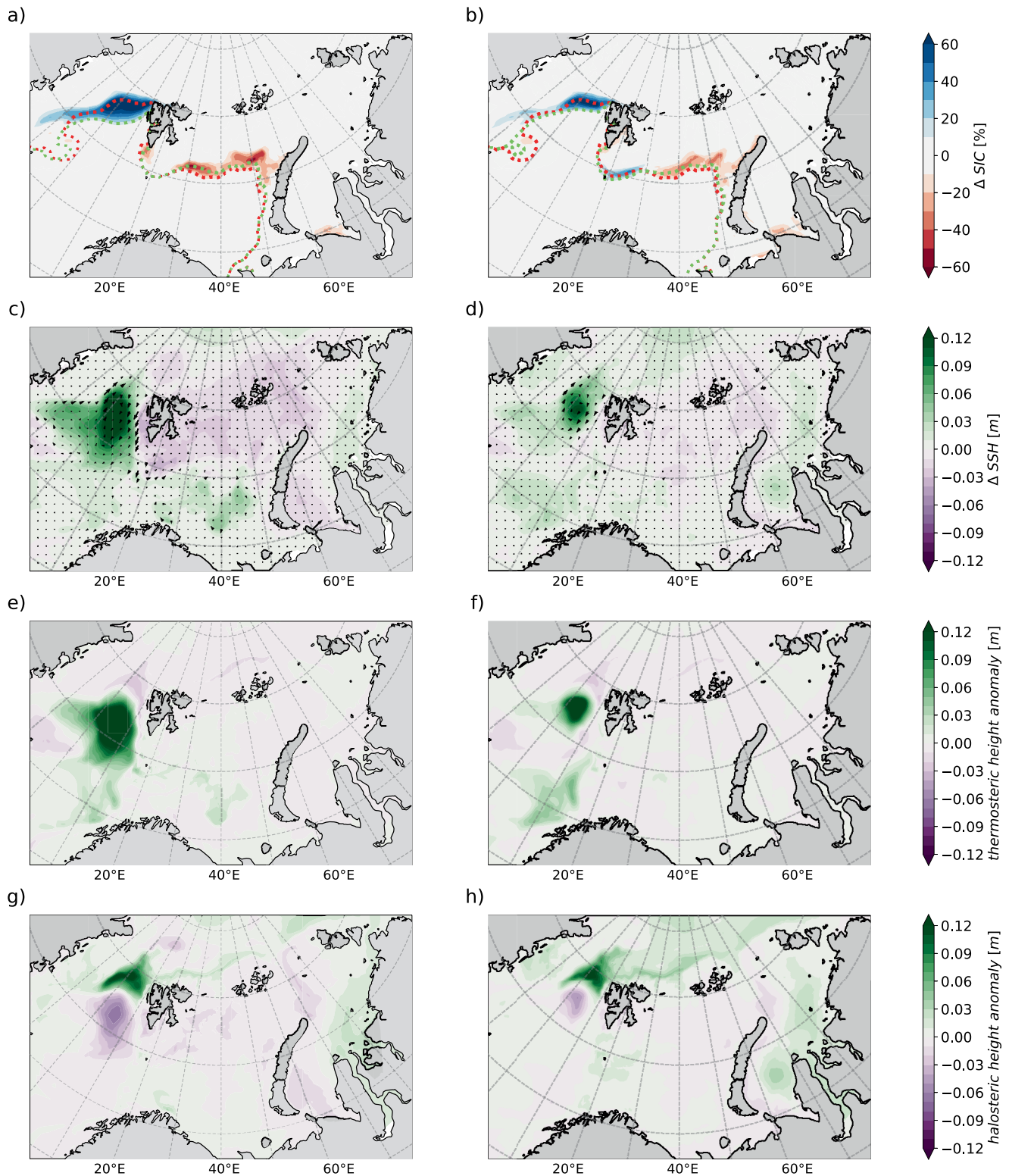
Figure 7. Anomalous winter (December-May) sea ice concentration (a, b), sea surface height (c, d), thermosteric height anomaly (e, f) and halosteric height anomaly (g, h) for ANOM-JRA (left column) and ANOM-CORE2 (right column) relative to CTRL. The dotted lines in (a and b) depict the sea ice edge (sea ice concentration = 15%) in CTRL (magenta) and ANOM-JRA/ANOM-CORE2 (green), respectively. Vector field in (c), and (d) qualitatively depicts anomalous flow at 25 m depth. Lines of latitude are drawn every 5°N starting at 70°N.
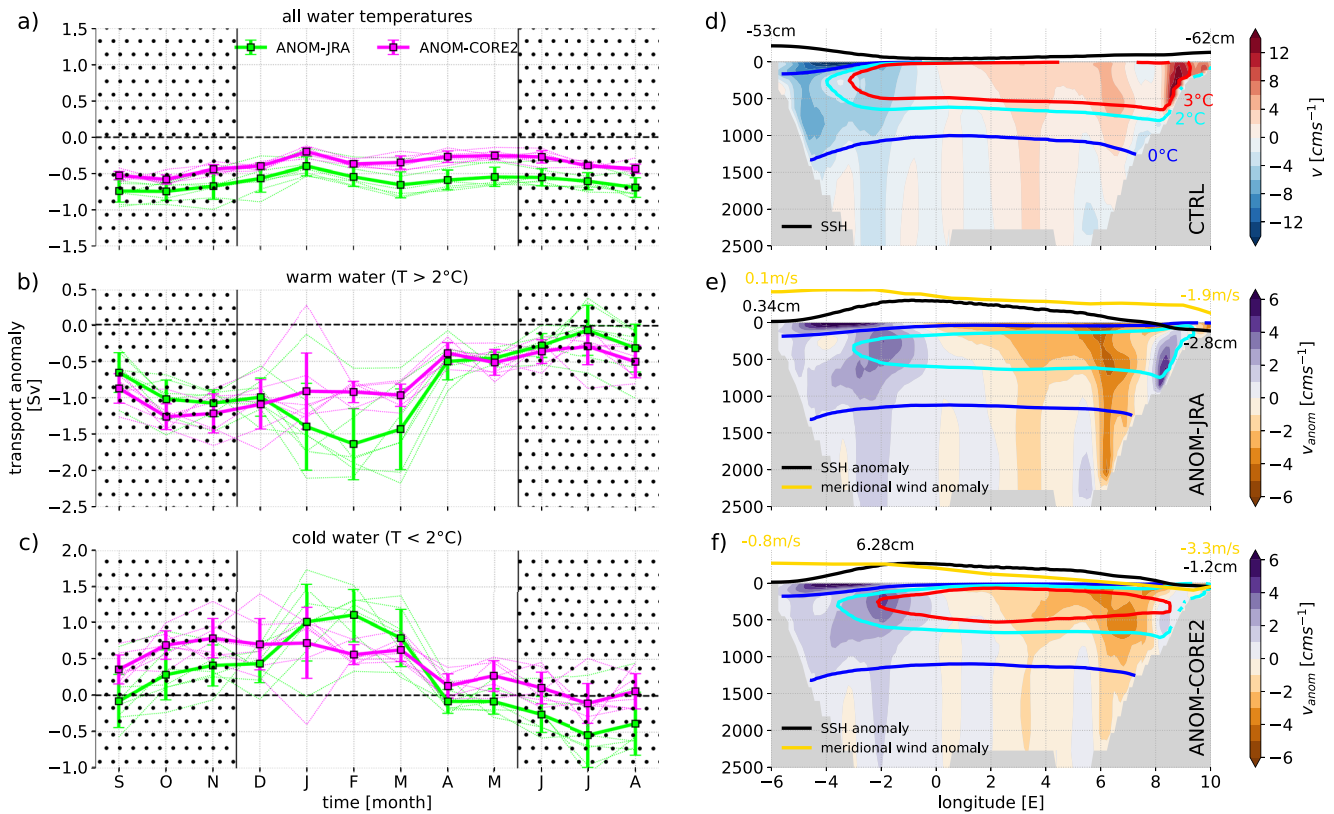
Figure 8. As in Figure 6 but for the Fram Strait section (78.8°N). Atlantic Water is defined as water with temperatures exceeding 2°C.

Atlantic Water flow through Fram Strait to reveal the impact of the wind anomaly on the Atlantic Water transport in this branch (Figure 8). When reaching Fram Stait, the Atlantic Water has already cooled substantially due to being exposed to the atmosphere for additional ∼900 km compared to the Atlantic Water in the Barents Sea Opening. Hence, 5°C is not an appropriate threshold as in the Barents Sea Opening anymore and we adjust the threshold for Atlantic Water in Fram Strait to 2°C (e.g., Hofmann et al., 2021; Wekerle, Wang, von Appen, et al., 2017).

As in the Barents Sea Opening, we observe a general modification of the net transport by about −0.5 Sv in the presence of the applied wind anomalies (Figure 8a). The poleward warm and saline Atlantic Water flow is reduced by approx. 1 Sv with a maximum reduction of 1.5 Sv during January, February, and March (Figure 8b). The cold southward flow of Polar Water is also reduced by up to 1 Sv during the same months as the Atlantic Water transport anomaly peaks (Figure 8c), yielding evidence for a general reduction of the water mass exchange through Fram Strait that is further investigated below. In both ANOM-JRA and ANOM-CORE2 three main adjustments in the transect at 78.8°N are observed (Figures 8e and 8f):

1. The whole barotropic circulation pattern, i.e., the southward flow between 6°W and 0°E and northward flow between 0°E and 10°E, is substantially weakened in the presence of the wind anomalies.
2. The temperature in the zonal transect at 78.8°N is reduced in the two perturbation runs.
3. The West Spitsbergen Current is shifted westwards toward deeper isobaths.

Here we propose a mechanism controlling the observed changes described above. By superimposing cyclonic wind anomalies, we add an additional source of wind stress curl to the northern Nordic Seas. The topographically guided West Spitsbergen Current flowing along the continental slope (f/H contours) is affected by the additional wind stress curl and shifts down the continental slope toward deeper isobaths to balance the additional potential vorticity source from the wind forcing. The shift of the West Spitsbergen Current toward deeper isobaths is illustrated in Figures 9a–9c. The westward shift toward deeper isobaths is observed in the temperature field as far upstream as 74.5°N. The more westward and deeper flow of the West Spitsbergen Current along the continental slope results in less Atlantic Water reaching 78.8°N latitude, leading to the cooling and reduced northward Atlantic Water transport in Fram Strait (Figure 8). A larger amount of Atlantic Water recirculates
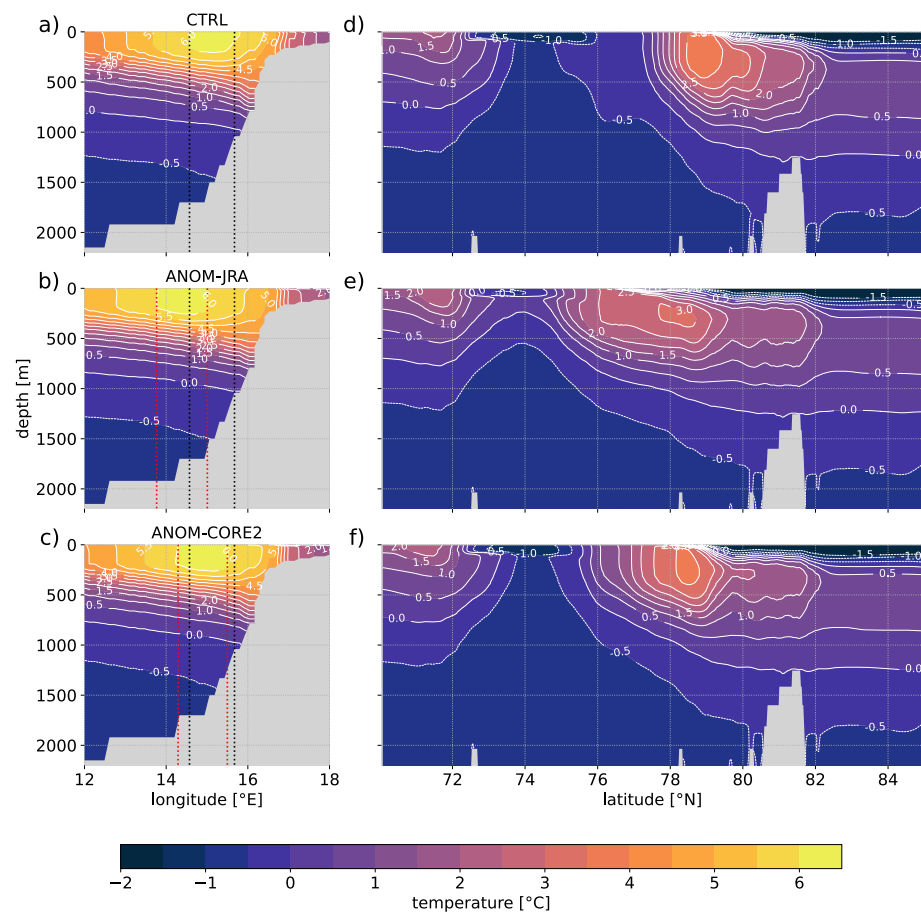
Figure 9. Temperature sections along 74.5°N and along 2°E for CTRL (a, d), ANOM-JRA (b, e), and ANOM-CORE2 (c, f). Black vertical lines in (a–c) depict zonal limits of the 6°C isotherm at 50 m depth in CTRL as a proxy for the location of the West Spitsbergen Current. Red lines in (b), and (c) depict the same but for ANOM-JRA (b), and ANOM-CORE2 (c).

westward at lower latitudes as shown in Figures 9d–9f. This increases the amount of Atlantic Water entering the Greenland Sea Gyre and causes a thermosteric rise in sea surface height that sets up an anticyclonic circulation anomaly counteracting the cyclonic Greenland Sea Gyre circulation (Figures 10b and 10c; Figures 7c and 7d). Along with the southward retreat of the recirculation branch of the Atlantic Water (Figures 9d–9f), the cold and fresh Arctic water masses expand to the south. This ocean condition reduces local sea ice melting and together with the anomalous southward wind contributes to the southward expansion of sea ice cover in Fram Strait (Figures 7a and 7b).

Our results suggest that the added wind perturbations impact the magnitude of Atlantic Water transport toward the Arctic Ocean in Fram Strait rather than via the Barents Sea Opening pathway. While we observe strong warming in the northern Greenland Sea Gyre and a pronounced cooling in Fram Strait in the perturbation simulations, we find that the Atlantic Water flow along the continental slope north of Spitsbergen at 300 m depth is cooler in ANOM-JRA (−1°C) and ANOM-CORE2 (−0.5°C) than in CTRL (Figures 10e and 10f). This cooling suggests that less oceanic heat is reaching the Arctic basin via Fram Strait in the presence of the applied cyclonic wind perturbations.

The reduced temperature west of 8°E in Fram Strait further increases the density gradient between the core of the West Spitsbergen Current and the interior of Fram Strait, which slightly strengthens the baroclinic current at about 8°E (Figure 8). However, this does not offset the reduction in the northward flow west of 8°E and the overall heat inflow toward the Arctic interior is reduced as indicated by the negative temperature anomaly at 300 m depth north of Spitsbergen (Figures 10b and 10c).
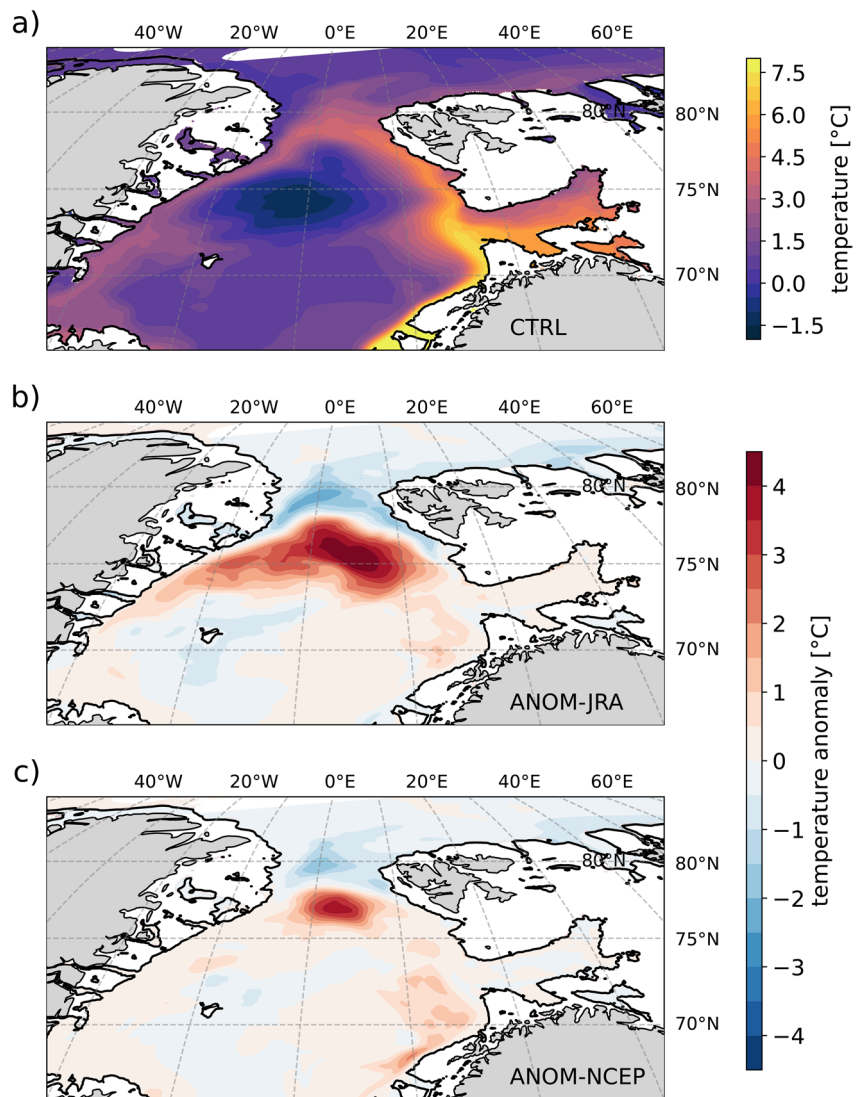
Figure 10. (a) Temperature at 300 m depth in CTRL. (b and c) Temperature anomaly at 300 m depth in ANOM-JRA and ANOM-CORE2, respectively. All plots show the winter mean (December-May) of the last model year. The black line depicts the 300 m isobath.

4. Discussion and Conclusions

We performed wind-perturbation experiments by applying wind anomalies in the Barents Sea and its vicinity to investigate the impact of local cyclonic wind perturbations caused by the local retreat of winter sea ice on Atlantic Water transport at the Barents Sea Opening and Fram Strait. We found that the Barents Sea Opening Atlantic Water inflow is not sensitive to local cyclonic wind anomalies. Therefore, our results suggest that the wind-feedback mechanism does not operate in the real world (in the current climate condition). It thus further seems unlikely that the wind feedback acts on stabilizing the Barents Sea warm phase as proposed by Ådlandsvik and Loeng (1991). Our high-resolution simulations, which can reasonably represent the details of the circulation in the studied region, confirm the conclusion of Smedsrud et al. (2013) who could not find any evidence for the existence of the wind feedback in their coupled simulation with a very coarse model resolution. Our study explains the reason.

The general sea surface height-anomaly pattern in the Barents Sea in our perturbation experiments is similar to the one presented by Lien et al. (2013), who found negative sea surface height anomalies covering the whole northern Barents Sea shelf driven by off-shelf Ekman transport as a result of cyclonic wind anomalies. The modification of

the sea surface height in the northern Barents Sea impacts the sea surface height gradient controlling the outflow of modified Atlantic Water and Polar Water south of Bear Island. The results of our study show that this impact is also present on annual and longer time scales. During periods of pronounced off-shelf transport, flow reversals of the westward-directed current at the Bear Island slope, transporting modified Atlantic Water, can be generated (Lien et al., 2013). However, in our perturbation simulations, we observe a substantial weakening, but not a reversal of the flow. This is because the persistent wind anomalies we used are weaker than the high-frequency wind variability studied by Lien et al. (2013), who attributed the increased frequency of flow reversals during winter to the vigorous low-pressure activity. Our study suggests that the strengthening of the cyclonic wind anomaly over the northern Barents Sea shelf in a warming climate could foster such flow-reversal events and possibly lead to a long-term trend in the currents over the Bear Island slope. The impact of the changes in cold water outflow through the Barents Sea Opening on sea ice and adjacent ocean conditions requires further dedicated studies. Based on the results presented in this study, as well as those of Lien et al. (2013), and Aue et al. (2022) who studied the impact of single transient cyclones on the local distribution of sea ice in the Barents Sea, we further suggest a more detailed study of the impact of synoptic-scale atmosphere variability on the Barents Sea Opening transports for future research.

Our study further suggests that the location of the wind anomaly is crucial with respect to whether and how it can significantly influence the ocean currents in the Barents Sea Opening. The cyclonic wind anomaly associated with the decline of Barents Sea sea ice in the last ~40 years, as we explored in this paper, can only strongly influence sea surface height in the northern part of the Barents Sea Opening and weaken the outflow of modified Atlantic Water. We further performed the same perturbation experiments with wind anomalies retrieved from the ERA5 and ERA interim reanalysis datasets. By using the various reanalysis products to generate the anomalies to perturb the model forcing, we already cover some variability in terms of shape, location, and magnitude of the anomalies that is found among the reanalysis products. The results of the additional experiments are, however, very similar to the ANOM-CORE and ANOM-JRA runs and do not provide evidence for the existence of the wind feedback. The consistent results of the four simulations give us confidence that the choice of the reanalysis product to generate the wind anomalies does not impact the overall conclusion. To influence the warm Atlantic Water inflow, a strong zonal wind anomaly located in the southern part of the Barents Sea Opening would be needed, which is not found in any of the considered wind anomalies associated with sea ice decline in reanalysis datasets.

As we use an ocean-sea ice model, the full feedback cannot operate in our simulations as the atmospheric forcing is prescribed and cannot adapt to changes in ocean and sea ice conditions. A study investigating a Nordic Seas wind feedback was carried out by Kovac et al. (2020) using a partially coupled model approach (Thoma et al., 2015) to identify cause and effect chains within a feedback loop related to the Nordic Seas. That approach, embedded in the framework of climate response functions as proposed by Marshall et al. (2017), might be helpful for studying the Barents Sea climate system. In this study, however, we focused on the Barents Sea Opening Atlantic Water import and its sensitivity to local wind forcing as a single but crucial component of the wind-feedback loop (as illustrated in Figure 2). We assessed the possibility of the occurrence of this wind feedback using reanalysis data in our perturbation experiments that represents the current climate condition. Therefore, we consider our approach sufficient to suggest that the previously proposed wind feedback is currently not functioning.

Our simulations also reveal strong impacts of the wind anomalies on the circulation in Fram Strait and the Greenland Sea Gyre. We propose that a change in the wind field in Fram Strait and the northern Nordic Seas can cause a down-slope shift of the West Spitsbergen Current, leading to less oceanic heat reaching the Arctic basin via Fram Strait pathway and an increased amount of Atlantic Water recirculating within the Greenland Sea Gyre. The recirculation branch of the Atlantic Water is shifted southward under the applied wind perturbations, allowing Polar Water to expand further to the south. While revealing the same tendencies in terms of redirected Atlantic Water flow in Fram Strait, the changes observed in ANOM-JRA are much more pronounced than in ANOM-CORE2. Although using different time periods for the generation of the wind perturbations due to limited data availability for NCEP-CORE2, the wind perturbations are very similar in magnitude as well as direction of the winds (Figures 5d and 5e). However, the largest differences between the two perturbations are found in the vicinity of the West Spitsbergen Current and the northwestern Barents Sea shelf. Our results highlight that winds in these regions can strongly affect the ocean currents. Hence, we suggest that a proper representation of the local winds in these specific regions (in reanalysis products and in coupled climate models) is crucial for simulating the Barents Sea and Fram Strait flow field and even small deviations have a large impact.

General warming of the Atlantic Water layer in the Arctic Ocean has been observed (e.g., Polyakov et al., 2013, 2017). This warming was due to the increase in both the Atlantic Water temperature and poleward ocean volume transport at Fram Strait, which was intensified by Arctic sea ice decline (Wang et al., 2020). The mechanism tending to reduce ocean heat inflow at Fram Strait identified in our study might not be dominating the trend, but could still exist and counteract the upward trend in ocean heat inflow.

Conflict of Interest

The authors declare no conflicts of interest relevant to this study.

Data Availability Statement

FESOM2.1 model source code can be accessed at https://github.com/FESOM/fesom2; NSIDC Sea Ice Index, Version 3 is freely available at https://nsidc.org/data/G02135/versions/3 (https://doi.org/10.7265/N5K072F8) the Japanese 55-year Reanalysis is provided at https://rda.ucar.edu/ (https://doi.org/10.5065/D6HH6H41) NCEP-CORE2 reanalysis data is provided at https://data1.gfdl.noaa.gov/ (https://doi.org/10.5065/D6WH2N0S) Transports in FESOM2 are computed with pyfesom2 (https://github.com/FESOM/pyfesom2); model output and settings needed to reproduce the results are stored at https://doi.org/10.5281/zenodo.7458143.

References

Aagaard, K., Foldvik, A., & Hillman, S. R. (1987). The west Spitsbergen current: Disposition and water mass transformation. *Journal of Geophysical Research*, *92*(C4), 3778–3784. https://doi.org/10.1029/JC092iC04p03778

Aagaard, K., & Greisman, P. (1975). Toward new mass and heat budgets for the Arctic Ocean. *Journal of Geophysical Research*, *80*(27), 3821–3827. https://doi.org/10.1029/JC080i027p03821

Ådlandsvik, B., & Loeng, H. (1991). A study of the climatic system in the Barents Sea. *Polar Research*, *10*(1), 45–50. https://doi.org/10.3402/polar.v10i1.6726

Årthun, M., Eldevik, T., & Smedsrud, L. H. (2019). The role of Atlantic heat transport in future Arctic winter sea ice loss. *Journal of Climate*, *32*(11), 3327–3341. https://doi.org/10.1175/JCLI-D-18-0750.1

Årthun, M., Eldevik, T., Smedsrud, L. H., Skagseth, Ø., & Ingvaldsen, R. B. (2012). Quantifying the influence of Atlantic heat on Barents Sea ice variability and retreat. *Journal of Climate*, *25*(13), 4736–4743. https://doi.org/10.1175/JCLI-D-11-00466.1

Aue, L., Vihma, T., Uotila, P., & Rinke, A. (2022). A new insights into cyclone impacts on sea ice in the Atlantic sector of the Arctic Ocean in winter. *Geophysical Research Letters*, *49*(22), e2022GL100051. https://doi.org/10.1029/2022GL100051

Barton, B. I., Lenn, Y. D., & Lique, C. (2018). Observed Atlantification of the Barents Sea causes the Polar Front to limit the expansion of winter sea ice. *Journal of Physical Oceanography*, *48*(8), 1849–1866. https://doi.org/10.1175/JPO-D-18-0003.1

Bengtsson, L., Semenov, V. A., & Johannessen, O. M. (2004). The early twentieth-century warming in the Arctic—A possible mechanism. *Journal of Climate*, *17*(20), 4045–4057. https://doi.org/10.1175/1520-0442(2004)017<4045:TETWIT>2.0.CO;2

Beszczynska-Möller, A., Fahrbach, E., Schauer, U., & Hansen, E. (2012). Variability in Atlantic Water temperature and transport at the entrance to the Arctic Ocean, 1997–2010. *ICES Journal of Marine Science*, *69*(5), 852–863. https://doi.org/10.1093/icesjms/fss056

Beszczynska-Möller, A., Woodgate, R. A., Lee, C., Melling, H., & Karcher, M. (2011). A synthesis of exchanges through the main oceanic gateways to the Arctic Ocean. *Oceanography*, *24*(3), 82–99. https://doi.org/10.5670/oceanog.2011.59

Boisvert, L. N., Petty, A. A., & Stroeve, J. C. (2016). The impact of the extreme winter 2015/16 Arctic cyclone on the Barents–Kara Seas. *Monthly Weather Review*, *144*(11), 4279–4287. https://doi.org/10.1175/MWR-D-16-0234.1

Bonan, D. B., Lehner, F., & Holland, M. M. (2021). Partitioning uncertainty in projections of Arctic sea ice. *Environmental Research Letters*, *16*(4), 044002. https://doi.org/10.1088/1748-9326/abe0ec

Bourke, R. H., Newton, J. L., Paquette, R. G., & Tunnicliffe, M. D. (1987). Circulation and water masses of the East Greenland Shelf. *Journal of Geophysical Research*, *92*(C7), 6729–6740. https://doi.org/10.1029/JC092iC07p06729

Bourke, R. H., Weigel, A. M., & Paquette, R. G. (1988). The westward turning branch of the West Spitsbergen Current. *Journal of Geophysical Research*, *93*(C11), 14065–14077. https://doi.org/10.1029/JC093iC11p14065

Cavalieri, D. J., & Parkinson, C. L. (2012). Arctic sea ice variability and trends, 1979–2010. *The Cryosphere*, *6*(4), 881–889. https://doi.org/10.5194/tc-6-881-2012

Comiso, J. C., Parkinson, C. L., Gersten, R., & Stock, L. (2008). Accelerated decline in the Arctic sea ice cover. *Geophysical Research Letters*, *35*(1), L01703. https://doi.org/10.1029/2007GL031972

Danilov, S., Sidorenko, D., Wang, Q., & Jung, T. (2017). The finite-volume sea ice–ocean model (fesom2). *Geoscientific Model Development*, *10*(2), 765–789. https://doi.org/10.5194/gmd-10-765-2017

De Steur, L., Hansen, E., Mauritzen, C., Beszczynska-Möller, A., & Fahrbach, E. (2014). Impact of recirculation on the East Greenland Current in Fram Strait: Results from moored current meter measurements between 1997 and 2009. *Deep Sea Research Part I: Oceanographic Research Papers*, *92*, 26–40. https://doi.org/10.1016/j.dsr.2014.05.018

Dmitrenko, I. A., Rudels, B., Kirillov, S. A., Aksenov, Y. O., Lien, V. S., Ivanov, V. V., et al. (2015). Atlantic water flow into the Arctic Ocean through the St. Anna trough in the northern Kara Sea. *Journal of Geophysical Research: Oceans*, *120*(7), 5158–5178. https://doi.org/10.1002/2015JC010804

England, M., Jahn, A., & Polvani, L. (2019). Nonuniform contribution of internal variability to recent Arctic sea ice loss. *Journal of Climate*, *32*(13), 4039–4053. https://doi.org/10.1175/JCLI-D-18-0864.1

Gerdes, R., Karcher, M. J., Kauker, F., & Schauer, U. (2003). Causes and development of repeated Arctic Ocean warming events. *Geophysical Research Letters*, *30*(19), 1980. https://doi.org/10.1029/2003GL018080

Graham, R. M., Itkin, P., Meyer, A., Sundfjord, A., Spreen, G., Smedsrud, L. H., et al. (2019). Winter storms accelerate the demise of sea ice in the Atlantic sector of the Arctic Ocean. *Scientific Reports*, *9*(1), 1–16. https://doi.org/10.1038/s41598-019-45574-5

Hofmann, Z., von Appen, W. J., & Wekerle, C. (2021). Seasonal and mesoscale variability of the two Atlantic Water recirculation pathways in Fram Strait. *Journal of Geophysical Research: Oceans*, *126*(7), e2020JC017057. https://doi.org/10.1029/2020JC017057

Ingvaldsen, R. B., Asplin, L., & Loeng, H. (2004). Velocity field of the western entrance to the Barents Sea. *Journal of Geophysical Research*, *109*(C3), C03021. https://doi.org/10.1029/2003JC001811

Kobayashi, S., Ota, Y., Harada, Y., Ebita, A., Moriya, M., Onoda, H., et al. (2015). The JRA-55 reanalysis: General specifications and basic characteristics. *Journal of the Meteorological Society of Japan. Ser. II*, *93*(1), 5–48. https://doi.org/10.2151/jmsj.2015-001

Kovács, T., Gerdes, R., & Marshall, J. (2020). Wind feedback mediated by sea ice in the Nordic Seas. *Journal of Climate*, *33*(15), 6621–6632. https://doi.org/10.1175/JCLI-D-19-0632.1

Large, W., & Yeager, S. G. (2009). The global climatology of an interannually varying air–sea flux data set. *Climate Dynamics*, *33*(2), 341–364. https://doi.org/10.1007/s00382-008-0441-3

Lien, V. S., Schlichtholz, P., Skagseth, Ø., & Vikebø, F. B. (2017). Wind-driven Atlantic Water flow as a direct mode for reduced Barents Sea ice cover. *Journal of Climate*, *30*(2), 803–812. https://doi.org/10.1175/JCLI-D-16-0025.1

Lien, V. S., Hjøllo, S. S., Skogen, M. D., Svendsen, E., Wehde, H., Bertino, L., et al. (2016). An assessment of the added value from data assimilation on modelled Nordic Seas hydrography and ocean transports. *Ocean Modelling*, *99*, 43–59. https://doi.org/10.1016/j.ocemod.2015.12.010

Lien, V. S., Vikebø, F. B., & Skagseth, Ø. (2013). One mechanism contributing to co-variability of the Atlantic inflow branches to the Arctic. *Nature Communications*, *4*(1), 1–6. https://doi.org/10.1038/ncomms2505

Lind, S., Ingvaldsen, R. B., & Furevik, T. (2018). Arctic warming hotspot in the northern Barents Sea linked to declining sea ice import. *Nature Climate Change*, *8*(7), 634–639. https://doi.org/10.1038/s41558-018-0205-y

Liu, Z., Risi, C., Codron, F., Jian, Z., Wei, Z., He, X., et al. (2022). Atmospheric forcing dominates winter Barents-Kara sea ice variability on interannual to decadal time scales. *Proceedings of the National Academy of Sciences of the United States of America*, *119*(36), e2120770119. https://doi.org/10.1073/pnas.2120770119

Marshall, J., Scott, J., & Proshutinsky, A. (2017). "Climate response functions" for the Arctic Ocean: A proposed coordinated modelling experiment. *Geoscientific Model Development*, *10*(7), 2833–2848. https://doi.org/10.5194/gmd-10-2833-2017

Onarheim, I. H., & Årthun, M. (2017). Toward an ice-free Barents Sea. *Geophysical Research Letters*, *44*(16), 8387–8395. https://doi.org/10.1002/2017GL074304

Polyakov, I. V., Bhatt, U. S., Walsh, J. E., Abrahamsen, E. P., Pnyushkov, A. V., & Wassmann, P. F. (2013). Recent oceanic changes in the Arctic in the context of long-term observations. *Ecological Applications*, *23*(8), 1745–1764. https://doi.org/10.1890/11-0902.1

Polyakov, I. V., Pnyushkov, A. V., Alkire, M. B., Ashik, I. M., Baumann, T. M., Carmack, E. C., et al. (2017). Greater role for Atlantic inflows on sea ice loss in the Eurasian Basin of the Arctic Ocean. *Science*, *356*(6335), 285–291. https://doi.org/10.1126/science.aai8204

Proshutinsky, A. Y., & Johnson, M. A. (1997). Two circulation regimes of the wind-driven Arctic Ocean. *Journal of Geophysical Research*, *102*(C6), 12493–12514. https://doi.org/10.1029/97JC00738

Schauer, U., Beszczynska-Möller, A., Walczowski, W., Fahrbach, E., Piechura, J., & Hansen, E. (2008). Variation of measured heat flow through the Fram Strait between 1997 and 2006. In *Arctic–subarctic ocean fluxes* (pp. 65–85). Springer. https://doi.org/10.1007/978-1-4020-6774-7_4

Schreiber, E. A., & Serreze, M. C. (2020). Impacts of synoptic-scale cyclones on Arctic sea-ice concentration: A systematic analysis. *Annals of Glaciology*, *61*(82), 139–153. https://doi.org/10.1017/aog.2020.23

Screen, J. A., & Simmonds, I. (2010). The central role of diminishing sea ice in recent Arctic temperature amplification. *Nature*, *464*(7293), 1334–1337. https://doi.org/10.1038/nature09051

Serreze, M. C., Barrett, A. P., Slater, A. G., Steele, M., Zhang, J., & Trenberth, K. E. (2007). The large-scale energy budget of the Arctic. *Journal of Geophysical Research*, *112*(D11), D11122. https://doi.org/10.1029/2006JD008230

Shu, Q., Wang, Q., Song, Z., & Qiao, F. (2021). The poleward enhanced Arctic Ocean cooling machine in a warming climate. *Nature Communications*, *12*(1), 1–9. https://doi.org/10.1038/s41467-021-23321-7

Sidorenko, D., Danilov, S., Koldunov, N., Scholz, P., & Wang, Q. (2020). Simple algorithms to compute meridional overturning and barotropic streamfunctions on unstructured meshes. *Geoscientific Model Development*, *13*(7), 3337–3345. https://doi.org/10.5194/gmd-13-3337-2020

Skagseth, Ø., Eldevik, T., Årthun, M., Asbjørnsen, H., Lien, V. S., & Smedsrud, L. H. (2020). Reduced efficiency of the Barents Sea cooling machine. *Nature Climate Change*, *10*(7), 661–666. https://doi.org/10.1038/s41558-020-0772-6

Smedsrud, L. H., Esau, I., Ingvaldsen, R. B., Eldevik, T., Haugan, P. M., Li, C., et al. (2013). The role of the Barents Sea in the Arctic climate system. *Reviews of Geophysics*, *51*(3), 415–449. https://doi.org/10.1002/rog.20017

Smedsrud, L. H., Halvorsen, M. H., Stroeve, J. C., Zhang, R., & Kloster, K. (2017). Fram Strait sea ice export variability and September Arctic sea ice extent over the last 80 years. *The Cryosphere*, *11*(1), 65–79. https://doi.org/10.5194/tc-11-65-2017

Smedsrud, L. H., Ingvaldsen, R., Nilsen, J. E., & Skagseth, Ø. (2010). Heat in the Barents Sea: Transport, storage, and surface fluxes. *Ocean Science*, *6*(1), 219–234. https://doi.org/10.5194/os-6-219-2010

Sorteberg, A., & Kvingedal, B. (2006). Atmospheric forcing on the Barents Sea winter ice extent. *Journal of Climate*, *19*(19), 4772–4784. https://doi.org/10.1175/JCLI3885.1

Spreen, G., de Steur, L., Divine, D., Gerland, S., Hansen, E., & Kwok, R. (2020). Arctic sea ice volume export through Fram Strait from 1992 to 2014. *Journal of Geophysical Research: Oceans*, *125*(6), e2019JC016039. https://doi.org/10.1029/2019JC016039

Steele, M., Morison, J. H., & Curtin, T. B. (1995). Halocline water formation in the Barents Sea. *Journal of Geophysical Research*, *100*(C1), 881–894. https://doi.org/10.1029/94JC02310

Steele, M., Morley, R., & Ermold, W. (2001). PHC: A global ocean hydrography with a high-quality Arctic Ocean. *Journal of Climate*, *14*(9), 2079–2087. https://doi.org/10.1175/1520-0442(2001)014<2079:PAGOHW>2.0.CO;2

Strass, V. H., Fahrbach, E., Schauer, U., & Sellmann, L. (1993). Formation of Denmark Strait Overflow water by mixing in the East Greenland Current. *Journal of Geophysical Research*, *98*(C4), 6907–6919. https://doi.org/10.1029/92JC02732

Thoma, M., Gerdes, R., Greatbatch, R. J., & Ding, H. (2015). Partially coupled spin-up of the MPI-ESM: Implementation and first results. *Geoscientific Model Development*, *8*(1), 51–68. https://doi.org/10.5194/gmd-8-51-2015

Wang, Q., Ricker, R., & Mu, L. (2021). Arctic sea ice decline preconditions events of anomalously low sea ice volume export through Fram Strait in the early 21st century. *Journal of Geophysical Research: Oceans*, *126*(2), e2020JC016607. https://doi.org/10.1029/2020JC016607

Wang, Q., Wang, X., Wekerle, C., Danilov, S., Jung, T., Koldunov, N., et al. (2019). Ocean heat transport into the Barents Sea: Distinct controls on the upward trend and interannual variability. *Geophysical Research Letters*, *46*(22), 13180–13190. https://doi.org/10.1029/2019GL083837

Wang, Q., Wekerle, C., Danilov, S., Koldunov, N., Sidorenko, D., Sein, D., et al. (2018). Arctic sea ice decline significantly contributed to the unprecedented liquid freshwater accumulation in the Beaufort Gyre of the Arctic Ocean. *Geophysical Research Letters*, *45*(10), 4956–4964. https://doi.org/10.1029/2018GL077901

Wang, Q., Wekerle, C., Wang, X., Danilov, S., Koldunov, N., Sein, D., et al. (2020). Intensification of the Atlantic water supply to the Arctic Ocean through Fram Strait induced by Arctic sea ice decline. *Geophysical Research Letters*, *47*(3), e2019GL086682. https://doi.org/10.1029/2019GL086682

Wekerle, C., Wang, Q., Danilov, S., Jung, T., & Schröter, J. (2013). The Canadian Arctic Archipelago throughflow in a multiresolution global model: Model assessment and the driving mechanism of interannual variability. *Journal of Geophysical Research: Oceans*, *118*(9), 4525–4541. https://doi.org/10.1002/jgrc.20330

Wekerle, C., Wang, Q., Danilov, S., Schourup-Kristensen, V., von Appen, W. J., & Jung, T. (2017). Atlantic Water in the Nordic Seas: Locally eddy-permitting ocean simulation in a global setup. *Journal of Geophysical Research: Oceans*, *122*(2), 914–940. https://doi.org/10.1002/2016JC012121

Wekerle, C., Wang, Q., von Appen, W. J., Danilov, S., Schourup-Kristensen, V., & Jung, T. (2017). Eddy-resolving simulation of the Atlantic Water circulation in the Fram Strait with focus on the seasonal cycle. *Journal of Geophysical Research: Oceans*, *122*(11), 8385–8405. https://doi.org/10.1002/2017JC012974

Yang, S., & Christensen, J. H. (2012). Arctic sea ice reduction and European cold winters in CMIP5 climate change experiments. *Geophysical Research Letters*, *39*(20), L20707. https://doi.org/10.1029/2012GL053338

Yang, X. Y., Yuan, X., & Ting, M. (2016). Dynamical link between the Barents–Kara sea ice and the Arctic Oscillation. *Journal of Climate*, *29*(14), 5103–5122. https://doi.org/10.1175/jcli-d-15-0669.1